Assignment of a kinetic component to electron transfer between iron–sulfur clusters FX and FA/FB) of Photosystem I

ARTICLE *in* BIOCHIMICA ET BIOPHYSICA ACTA · DECEMBER 2006

Impact Factor: 4.66 · DOI: 10.1016/j.bbabio.2006.06.016 · Source: PubMed

7 AUTHORS, INCLUDING:

Martin Byrdin
Atomic Energy and Alternative Energies Co…
37 PUBLICATIONS **1,202** CITATIONS
SEE PROFILE

Stefano Santabarbara
Italian National Research Council
53 PUBLICATIONS **904** CITATIONS
SEE PROFILE

Kevin Redding
Arizona State University
82 PUBLICATIONS **2,313** CITATIONS
SEE PROFILE

Fabrice Rappaport
Institute of Physical and Chemical Biology
129 PUBLICATIONS **4,398** CITATIONS
SEE PROFILE

Available online at www.sciencedirect.com
ScienceDirect
Biochimica et Biophysica Acta 1757 (2006) 1529–1538
BIOCHIMICA ET BIOPHYSICA ACTA
BBA
www.elsevier.com/locate/bbabio

Assignment of a kinetic component to electron transfer between iron–sulfur clusters F_X and $F_{A/B}$ of Photosystem I

Martin Byrdin [a,1], Stefano Santabarbara [b], Feifei Gu [c], Wendy V. Fairclough [b], Peter Heathcote [b], Kevin Redding [c], Fabrice Rappaport [a,*]

[a] Institut de Biologie Physico-Chimique, UMR 7141 CNRS/Paris 6, 13 Rue Pierre et Marie Curie, 75005 Paris, France
[b] School of Biological Sciences, Queen Mary, University of London, Mile End Road, London, E1 4NS, UK
[c] Departments of Chemistry and Biological Sciences, University of Alabama, 206 Shelby Hall, 500 Campus Dr., Tuscaloosa, AL 35487, USA

Received 30 March 2006; received in revised form 14 June 2006; accepted 16 June 2006
Available online 12 July 2006

Abstract

We studied the kinetics of reoxidation of the phylloquinones in *Chlamydomonas reinhardtii* Photosystem I using site-directed mutations in the PhQ_A-binding site and of the residues serving as the axial ligand to $ec3_A$ and $ec3_B$ chlorophylls. In wild type PS I, these kinetics are biphasic, and mutations in the binding region of PhQ_A induced a specific slowing down of the slow component. This slowing allowed detection of a previously unobserved 180-ns phase having spectral characteristics that differ from electron transfer between phylloquinones and F_X. The new kinetic phase thus reflects a different reaction that we ascribe to oxidation of F_X^- by the $F_{A/B}$ FeS clusters. These absorption changes partly account for the differences between the spectra associated with the two kinetic components assigned to phylloquinone reoxidation. In the mutant in which the axial ligand to $ec3_A$ (PsaA–Met688) was targeted, about 25% of charge separations ended in $P_{700}^+A_0^-$ charge recombination; no such recombination was detected in the B-side symmetric mutant. Despite significant changes in the amplitude of the components ascribed to phylloquinone reoxidation in the two mutants, the overall nanosecond absorption changes were similar to the wild type. This suggests that these absorption changes are similar for the two different phylloquinones and that part of the differences between the decay-associated spectra of the two components reflect a contribution from different electron acceptors, i.e. from an inter-FeS cluster electron transfer.

Photosystem I (PS I) is a pigment–protein complex involved in the photosynthetic process. The three-dimensional structure of PS I from the cyanobacterium *Thermosynechococcus elongatus* [1] and from *Pisum sativum* [2] has been solved with a resolution of 2.5 Å and 4.5 Å, respectively. In both cases, it shows a core formed of the two large subunits, PsaA and PsaB, surrounded by a fence of several small subunits and covered on the stromal side by the PsaC, PsaD and PsaE subunits (see [3] for a review). PS I utilizes light energy to transfer electrons across the thylakoid membrane against a transmembrane electrochemical potential. Light is harvested by an antenna system arranged mainly along the membrane surfaces in a ring-like structure around the pseudo-symmetry axis between PsaA and PsaB onto which the electron transfer cofactors are threaded. These are, in order going from lumen to stroma (see Fig. 1A): P_{700}, a chlorophyll (Chl) a-Chl a′ dimer, two pairs of symmetrically arranged Chls, ($ec2_A/ec3_A$ and $ec2_B/ec3_B$, associated with the primary acceptor "A_0"), a pair of phylloquinones (PhQ_A, PhQ_B, the secondary acceptor "A_1"), the Fe_4S_4 cluster F_X, all bound by PsaA and PsaB, and finally, two other Fe_4S_4 clusters F_A and F_B, both bound by PsaC (in this study, F_A and F_B will not be distinguished and referred to as $F_{A/B}$). On the way from P_{700} to F_X, two branches of cofactors are arranged in a highly symmetric structure with respect to the axis defined by P_{700} and F_X (Fig. 1).

In intact PS I, the initial electron transfer steps to PhQ proceed on the picosecond timescale, whereas the subsequent electron transfer through PS I occurs in the tens to hundreds of

Abbreviations: A_0 (A_0^-), primary electron acceptor in PS I (a chlorophyll a) in the oxidized (reduced) state; A_1(A_1^-), secondary electron acceptor in PS I (a phylloquinone) in the oxidized (reduced) state; Chl *a*, chlorophyll *a*; Chl a′, C-13 epimer of Chl *a*; DAS, decay associated spectrum spectra; ET, electron transfer; FeS, iron–sulfur cluster; F_X, F_A and F_B, three [4Fe–4S] clusters in PS I; P_{700} (P_{700}^+), primary electron donor of PS I in the reduced (oxidized) state; PhQ, phylloquinone; PS I, photosystem I; WT, wild-type control strain

* Corresponding author. Tel.: +33 158 415 059; fax: +33 158 415 022.
E-mail address: Fabrice.Rappaport@ibpc.fr (F. Rappaport).
[1] Permanent address: CEA/Saclay, SBE bat 532, 91191Gif-sur-Yvette Cedex.

0005-2728/$ - see front matter © 2006 Elsevier B.V. All rights reserved.
doi:10.1016/j.bbabio.2006.06.016

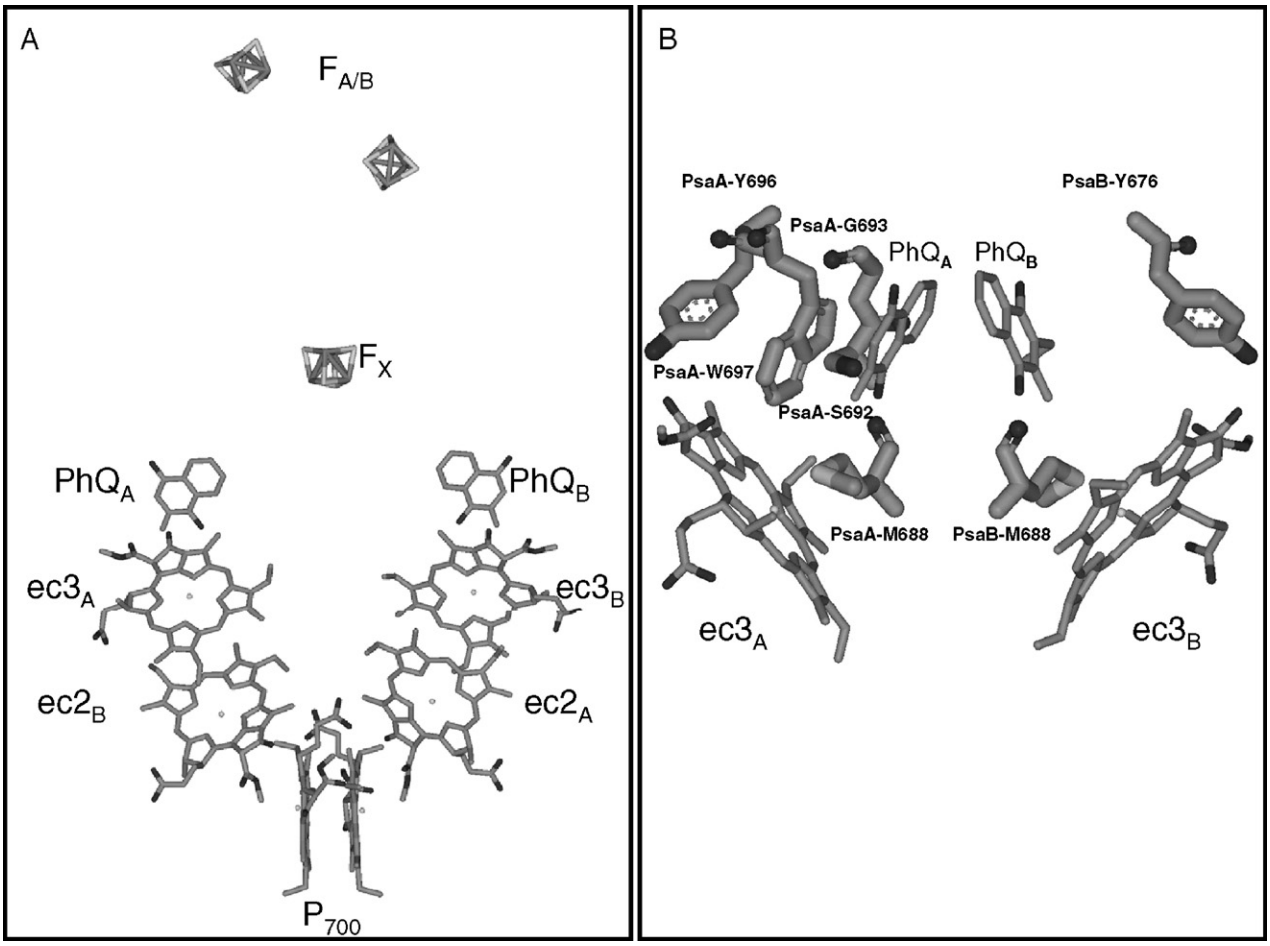

Fig. 1. Arrangement of the redox cofactors in PS I. Panel A: overall arrangement showing the two branches. Panel B: Close-up view of the $ec3_A$, $ec3_B$ and PhQ_A and PhQ_B regions showing the residues targeted by mutations in this study along with the cofactors affected. In the A branch, Tyr696 forms an H-bond to $ec3_A$, Met688 provides the axial ligand to $ec3_A$, Ser692 provides an H-bond to Trp697 that is π-stacked to PhQ_A. In the B branch, Tyr676 forms an H-bond to $ec3_A$, Met668 provides the axial ligand to $ec3_B$. This scheme was drawn using the coordinates deposited in the 1JB0 pdb file by Jordan et al. [1].

nanoseconds time range (see [4–6] for reviews). When bound to its docking site, the soluble electron acceptor ferredoxin or flavodoxin is reduced by the terminal bound FeS clusters in the sub-μs time range [7].

Nanosecond UV absorption changes in PS I have consistently yielded biphasic kinetics with time constants of about 25 and 250 ns (reviewed in [8]). Although PS I purification using harsh detergents such as Triton may increase the amplitude of the fast phase [9,10], its assignment to a purification artifact was ruled out when biphasic kinetics were also observed in whole cells [11]. Site-directed mutagenesis of the PhQ_A and PhQ_B binding sites led to the assignment of the fast and slow phases to the reoxidation of PhQ_B^- and PhQ_A^-, respectively. This was based on the finding that the mutations close to PhQ_A induced a slowing down of the slow phase, whereas those close to PhQ_B slowed down the fast phase, both without affecting the relative amplitudes of the components [12,13]. The assignment of the ~250-ns component to the reoxidation of PhQ_A^- is in agreement with the finding that the decay of the electron spin-polarized signal associated with the $[P_{700}^+A_{1A}^-]$ radical pair is slowed by the PsaA–W697H or PsaA–W697L mutations [14]. Interestingly, the absorption changes associated with the two PhQ reoxidation components are significantly different in the near UV and visible range in PS I from *Chlamydomonas reinhardtii* or *Synechocystis* sp. PCC 6803 [8,15–17]. When first observed, the differences in the DAS of the fast and slow component were interpreted along the lines of a model according to which the fast phase would reflect reoxidation of PhQ^- by F_X and the slow one electron transfer from F_X to $F_{A/B}$ [15]. According to this model, the ET reaction between PhQ^- and F_X has a low equilibrium constant so that a significant fraction of PhQ^- is reoxidized concomitantly with ET from F_X^- to $F_{A/B}$ [9]. In this framework, the absorption changes associated with the two phases are expected to be different as they reflect different spectral contributions associated with the two reactions. Meanwhile, the premise that only one out of the two PhQs is reduced has been weakened by the effects of the site directed mutation in the vicinity of either PhQ_A or PhQ_B. Still, the spectroscopic differences remain and are not accounted for by the assignment of the slow and fast phases to ET from PhQ_A^- to F_X and PhQ_B^- to F_X, respectively.

The present work addresses this issue in the light of the study of two classes of site-directed PS I mutants from *Chlamydomonas reinhardtii*: the PsaA–S692A and PsaA–G693W mutants, which affect the PhQ_A binding site, and the PsaA–

M688L/H and PsaB–M668H mutants, in which the axial ligands to $ec3_A$ or $ec3_B$ have been modified. For ease of comparison with the structure (see also Fig. 1B), all residues are referred to using the numbering from *Thermosynechococcus elongatus*.

1. Material and methods

1.1. Strains

Site-directed changes creating the PsaA–M688L or PsaA–M688H and PsaB–M668H mutations were introduced into the *psaA* and *psaB* genes by biolistic transformation of the wild-type *C. reinhardtii* strain CC-1021 as described previously [18]. These mutants were crossed to P71-17 (LHC-deficient, a gift from J. Girard-Bascou, Institut de Biologie Physico-Chimique, Paris) for nanosecond transient absorption measurements, and tetrad dissection carried out as described by Harris [19]. The PhQ_A-site mutations were created by PCR and introduced into *C. reinhardtii* using a previously established system [20]. Mutants were constructed in a genetic background lacking PSII due to the FUD7 (*psbA*Δ) mutation and most of the LHC complement due to the P71 mutation, to simplify spectroscopic analysis.

1.2. Transient absorption spectroscopy

Cells of *C. reinhardtii* were grown on Tris–acetate–phosphate medium at 25 °C under low light (6 μE m^{-2} s^{-1}), centrifuged and resuspended in 20 mM HEPES (pH 7.2) containing 20% Ficoll and 5 μM carbonylcyanide *p*-trifluoromethoxy-phenylhydrazone (FCCP). Detection of absorption changes in whole cells of *C. reinhardtii* in the ns to μs time regime and the 320–470 nm wavelength range was performed using a home-built two-beam, two-color pump-probe laser spectrometer, basically as described in [21], but using a Nd:YAG-driven frequency-doubled optical parametric oscillator (Panther, Continuum) to provide monochromatic (FWHM <5-cm^{-1}) detection pulses of <5-ns duration. Non-saturating excitation flashes at 700 nm were used to minimize antenna artifacts. A global fit procedure implemented in Mexfit [22] was used to describe the kinetic traces as the sum of up to four exponentials and a constant. The spectra shown in this work are the amplitudes of these exponential decay phases plotted as a function of wavelength.

2. Results

2.1. Effects of the PsaA–M688L, PsaA–M688H and PsaB–M668H mutations

We have measured the flash-induced transient absorption changes between 5 ns and 20 μs in the 320–460 nm range. Substituting the Met that provides the axial ligand to $ec3_A$ or $ec3_B$ [1] significantly altered the kinetics in this time range. As shown in Byrdin et al. [23], at 380 nm, where absorption changes associated with PhQ^- reoxidation predominate, the initial slopes of the kinetics in the PsaA–M688L or PsaA–M688H mutants were steeper than in the WT control strain, while they were less steep than WT in the PsaB–M668H mutant. This suggests that either the lifetime of the fast phase or its amplitude is increased (or decreased) when the PsaA–Met688 (or PsaB–Met668) residue is targeted. Consistent with the latter hypothesis, the kinetics of all four samples could be satisfactorily fitted with two exponentials having decay times of ~25 ns ("fast" phase) and ~250 ns ("slow" phase), but with different amplitudes in the different samples. To further characterize the effects of the mutations, we determined the decay-associated spectra of these components. The kinetics were globally fitted by a sum of three exponentials, two nanosecond phases and one with $\tau \approx 6$ μs, which is ascribed to the re-reduction of P_{700}^+ by bound plastocyanin. The amplitude of this 6-μs component was used as an internal standard for normalization of the spectra to the same amount of long-lived P_{700}^+. Fig. 2 shows the normalized spectra of the three exponential decay phases along with the initial absorption changes extrapolated to time zero (the initial spectrum) for the four strains. Although the lifetimes are similar in all cases (see Table 1), considerable changes in the amplitudes of the two sub-μs components are observed (compare Fig. 2C and D). In the A-side mutants, the amplitude of the fast phase was increased whereas that of the slow phase was decreased. Conversely, in the B-side mutant the amplitude of the slow phase was increased and that of the fast phase decreased. Besides these general trends, the DAS of both the fast and slow phases were significantly altered by the PsaA–M688H/L mutations in the 420–450 nm region, where they show a pronounced bleaching. This feature was not observed in the PsaB–M668H mutant (Fig. 2C, D). Furthermore, although the amplitudes of the slow component were different for the three strains above 360 nm, they were similar below 360 nm. The observation that mutation-induced changes in the amplitude of the slow component are wavelength dependent is not unprecedented. Indeed, Li et al. [24] already observed that mutation of PsaA–Tyr696 or PsaB–Tyr676 (involved in a H-bond with the 13-keto group of $ec3_A$ or $ec3_B$, respectively) resulted in significant changes in the amplitude of the fast and slow components above 360 nm, but much less pronounced below 360 nm for the slow component (see Fig. 3D in [24]). A possible explanation for this phenomenon is that the slow component does not solely reflect electron transfer between PhQ_A^- and F_X but also contains an additional contribution from another electron transfer reaction. Indeed, if two reactions involving different electron donors and acceptors occur concomitantly, the two reactions will be kinetically indistinguishable and the resulting decay-associated spectra will be a linear combination of the absorption changes resulting from each of these two reactions. In this framework, the PsaA–M688H and PsaB–M668H mutations could change the relative weight of one of these contributions (as observed above 360 nm) without significantly affecting the relative weight of the other (as seen below 360 nm). A possible strategy to check whether two different ET reactions do occur concomitantly is to slow down one of them specifically. For this reason we studied two mutants (PsaA–S692A and PsaA–G693W) in which the environment of PhQ_A is modified, as such mutations have been reported to specifically slow down the transient absorption changes associated with ET between PhQ_A and F_X [12–14].

2.2. Effects of the PsaA–S692A and PsaA–G693W mutations

Fig. 3A shows the kinetics of absorption changes at 380 nm for the WT and the two mutants in the vicinity of PhQ_A, along with sum-of-exponential fits of the data. We could not fit them by a stretched exponential model, because the lifetimes are too separate to be accounted for even by a wide distribution of

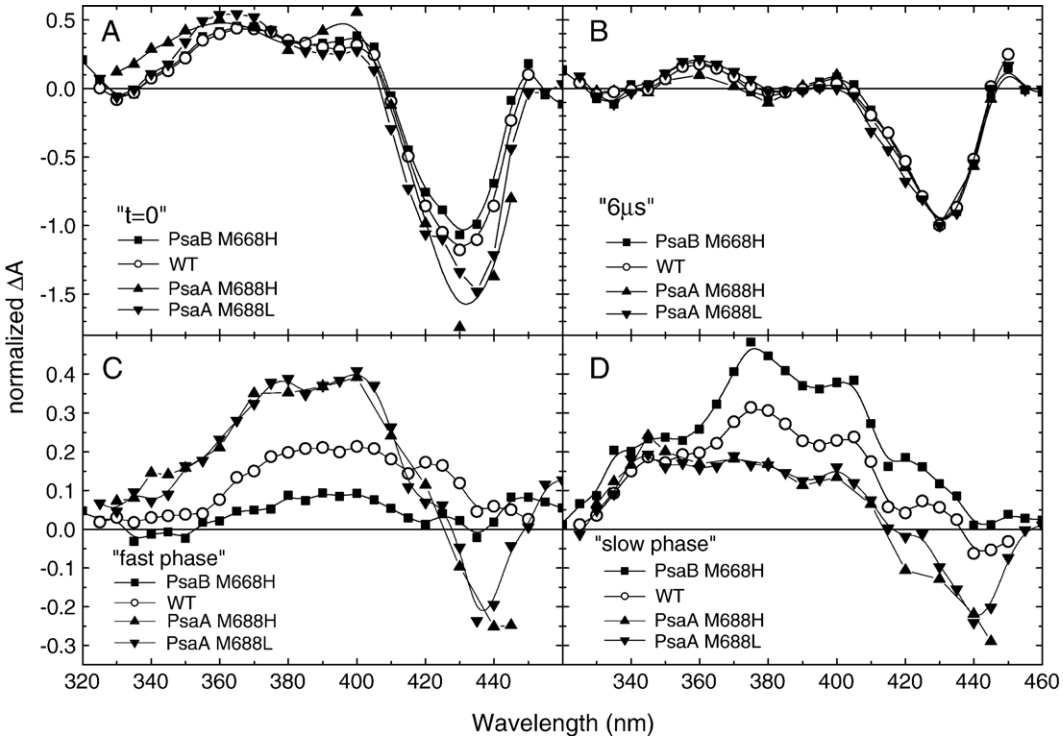

Fig. 2. Globally fitted amplitudes (symbols) of absorption changes in *C. reinhardtii* cells in wild type samples (WT), and different ec3 mutants: PsaB–M668H, PsaA–M688H, PsaA–M688L. Panel A: initial amplitudes; Panel B: 6-µs phase, the absolute values of the absorption changes associated with this phase were ~3–4 mOD at 430 nm; Panel C: fast nanosecond phase (~25 ns time constant); Panel D: slow nanosecond phase (~250 ns time constant). Lines are just splines through the data points. In panels C and D, the curves for PsaB–M668H are omitted for clarity since they would be similar to those corresponding to the PsaB–M668L mutant. For each strain, the DAS of the 6-µs was arbitrarily normalized to −1 at 430 nm and the normalization factor was then applied to the three other spectra (initial amplitude, 25-ns and 250-ns DAS). The various spectra are thus comparable, in all four panels, since they yield the amplitude of the various components for the same amount of P_{700}^{+} decaying with a time constant of 6 µs.

lifetimes. In both mutants, the slow phase was significantly slowed down, as observed previously in the case of the PsaA–W697F mutation, which also targeted the PhQ_A pocket [12]. The rate and amplitude of the fast component were unchanged in the two mutants.

Fig. 3B shows transient absorption changes at 445 nm for the 3 strains along with the fit. This wavelength was empirically chosen to minimize the absorption changes associated with either of the two nanosecond phases or with the 6-µs component (compare the absorbance scales of Fig. 3A and B). In the two mutant strains we observed an absorption decay between ~0.5 and 10 µs with the same decay rate observed at 380 nm, indicating that the (slowed) $PhQ_A \rightarrow F_X$ component has some

Table 1
Global fitting parameters for the mutants affecting $ec3_A$ or $ec3_B$

Strain	Exponential decay time (τ) of the three kinetic components			Relative amplitude of the fast component at 380 nm
WT	25±2 ns	250±15 ns	5.8±0.2 µs	40%
PsaA–M688H	18±2 ns	260±20 ns	7.3±0.4 µs	76%
PsaA–M688L	16±3 ns	216±25 ns	5.7±0.4 µs	69%
PsaB–M668H	24±2 ns	324±40 ns	5.6±0.4	17%
PsaA–Y696F[a]	22±3 ns	230±23 ns	5.3±0.3 µs	64%
PsaB–Y676F[a]	20±3 ns	220±25 ns	6.2±0.4 µs	17%

[a] Taken from [24].

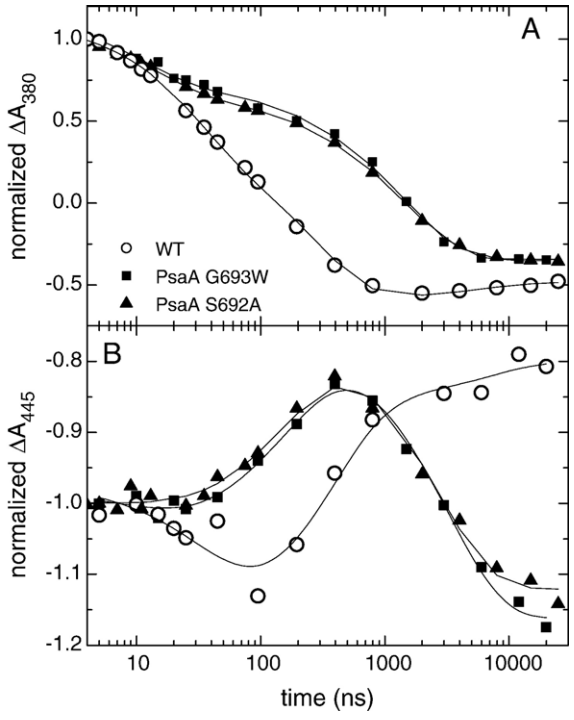

Fig. 3. Kinetics of normalized absorption changes at 380 nm (A) and 445 nm (B) between 5 ns and 20 µs (symbols) along with a three exponential fit with time constants of 25 ns, 250 ns, and 6 µs for the WT and four exponential fit with time constants indicated in the text for the two PhQ_A pocket mutants.

positive amplitude at this wavelength. We could also observe an absorption *increase* developing in the hundreds of ns time range. As shown in Fig. 3B, this absorption increase was observed in both the PsaA–S692A and PsaA–G693W mutants. The comparison with the kinetics of absorption changes at 380 nm (Fig. 3A) suggests the occurrence of three kinetically distinct events developing in the 5–30 ns, 40–300 ns and 400 ns-3 μs time window, respectively. In order to determine the DAS and time constant of each of these three components, we performed a global fitting of the kinetics measured with these two strains with four exponential phases, rather than three (see Fig. 4). In the PsaA–S692A mutant, this global fit yielded time constants of 15 ns, 180 ns, 1.1 μs ns and 5.8 μs. In the PsaA–G693W mutant, they were 12 ns, 185 ns, 1.5 μs ns and 6 μs. Based on its DAS (Fig. 4) and decay rate, the 6-μs component is assigned to the reduction of P_{700}^{+} by bound plastocyanin, as in the WT. The DAS of the first (~15 ns) and third (~1 μs) components are similar to those obtained in the WT for the fast and slow phases assigned to PhQ^{-} reoxidation. The amplitudes and shapes of these two DAS are hardly changed with respect to the corresponding WT DAS, suggesting that the slow phase is specifically slowed down by both PhQ_A site mutations.

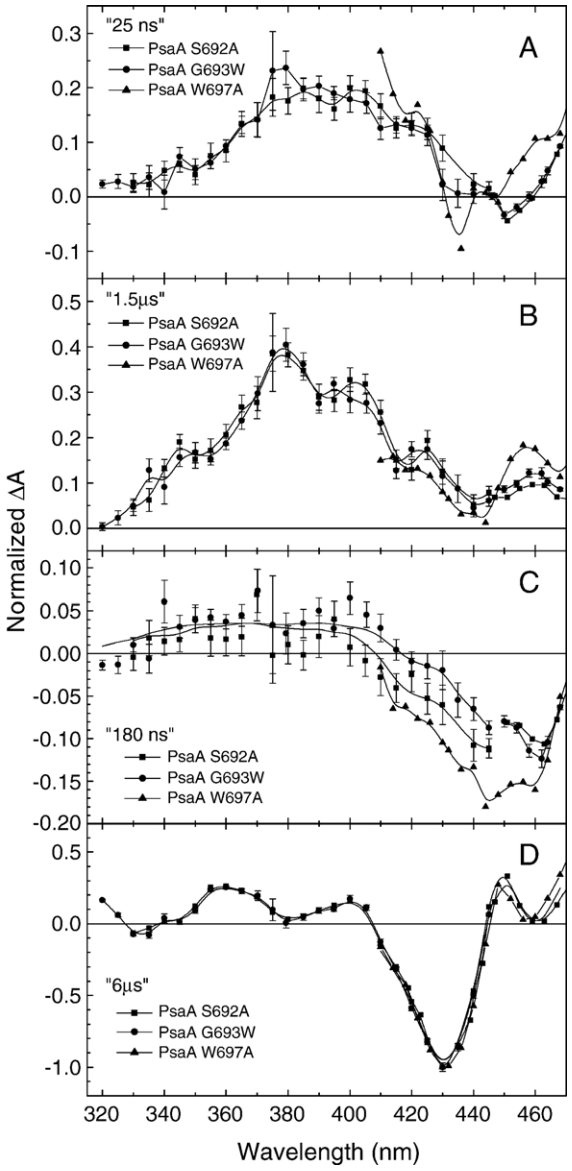

Fig. 4. Globally fitted amplitudes (panel A: 25 ns phase, panel B: 1.5 μs phase, panel C: 180 ns phase and panel D: 6 μs phase) of four components of absorption changes in *C. reinhardtii* cells of three different PhQ_A mutants (squares PsaA–S692A, circles PsaA–G693W and triangles PsaA–W697A, in the latter case the explored wavelength range was restricted to 410 nm to 470 nm). The absolute value of the absorption changes associated with the 180 ns phase were ~0.3–0.4 mOD at 460 nm. Lines are just splines through the data points.

The DAS of the intermediate component ($\tau \approx 180$ ns) does not display any features that could lead to its assignment to PhQ^{-} reoxidation. Consistent with the data obtained at 445 nm, this DAS is negative above 410 nm, leading to an absorption increase during its decay, whereas it is slightly positive below 410 nm. The fact that the decay rates and shape of the DAS of this intermediate component are essentially identical in the two PhQ_A site mutants demonstrates that they are not mutation-specific artifacts. This is further supported by the finding of similar trends in another PhQ_A site mutant, PsaA–W697A. The nature of the process represented by this new component will be discussed below.

3. Discussion

Recently, the question as to whether both cofactor branches are active for electron transfer in PS I has been a matter of some debate. Although it is widely agreed that the slower nanosecond decay component reflects reoxidation of PhQ_A^{-}, the assignment of the faster phase has been a point of contention. Until now, two main strategies have been pursued to address this question: making site-directed mutations in the PhQ_B binding pocket or near upstream cofactors in the B-branch. Whereas the former may be expected to specifically affect ET *from* PhQ_B, the latter should alter ET *to* PhQ_B. In *C. reinhardtii* both predictions were met. Mutations in the PhQ_B binding pocket specifically slowed down the rate of the fast phase [12]. Mutations of the PsaB–Tyr696 residue, involved in a H-bond with the 13-keto group of the $ec3_B$ Chl resulted in a decreased amplitude of the fast component, proposed to reflect a decreased PhQ_B reduction yield [24]. A similar effect is reported here for the PsaB–M668H mutant. Mutations of the axial ligand to the central Mg^{2+} of the $ec3_B$ Chl altered ET from $ec3_B$ to PhQ_B, yet still allowed photosynthetic growth at very low light intensity [18]. In *Synechocystis* sp. PCC 6803, however, similar mutations did not result in any significant changes, as seen by transient EPR measurements at room temperature [13,25] or ultra-fast optical spectroscopy [26]. Although there might be differences between PS I from different species, in *C. reinhardtii* most of the literature data may be interpreted in terms of a model in which both branches are active (see [6,8] for reviews). We will adopt this view and interpret the present data in this framework. It should also be pointed out that the decay-associated spectra might not always represent the pure absorption spectra (species associated spectra, SAS) of the cofactors involved in a particular electron transfer reaction (see [6] for a discussion). However in order to extract the SAS, a model-based analysis of the optical transients is

required. Such a procedure is much more demanding in terms of the number of fit parameters compared to the simpler description based on the exponential fitting of experimental data. Therefore in the following we will limit the discussion to the DAS.

3.1. The PsaA–Met688, but not the PsaB–Met668, mutation induces recombination of the primary radical pair $P^+_{700}A^-_0$

Site-directed mutations of the axial ligand to the two ec3 chlorophylls result in a decrease of the relative amplitude of the ~250-ns decay component of PhQ reoxidation in the PsaA–M684H/L mutants, and of the ~25 ns decay component in the PsaB–M664H mutant. Even though the relative proportion between the fast and the slow phase of PhQ reoxidation were selectively altered by the mutations, the characteristic time constants of the reoxidation kinetics were not significantly affected (Table 1). Substitution of the axial ligand to the central Mg^{2+} of the ec3 Chl with a Leu or a His is expected to alter the ec3 Chl redox potential. The weaker the ligand, the more negative the redox potential should be, but in the absence of detailed knowledge of the ligation state of the Mg^{2+} in the mutants, no reliable predictions can be made either on the direction or on the magnitude of the shift, rendering difficult the discussion of the rationale for the observed changes. Furthermore, the DAS of the nanosecond components displayed a marked trough in the 435–445 nm region in the two $ec3_A$ mutants, indicating the contribution of an additional event. In contrast, the shapes of the DAS were unaffected by the PsaB–M668H mutation. After normalization to the amplitude of the 6-μs component (at 430 nm), the amplitude of the absorption changes around 430 nm extrapolated to $t=0$ was larger in the $ec3_A$ mutants than in the WT or PsaB–M668H mutant. These two findings suggest that, in a fraction of the PsaA–Met688 mutant PS1 reaction centers, P^+_{700} decays in the sub-μs time domain. The spectroscopic signature of this decay (i.e. the trough in the 435–445 nm region) resembles the ($P^+_{700}A^-_0$–$P_{700}A_0$) spectrum reported by various authors [27,28], who showed that the (A^-_0–A_0) spectrum displays a bleaching minimum at ~438 nm. On this basis, we ascribe this decay to charge recombination of the $P^+_{700}A^-_0$ state, which occurs in WT with a halftime ranging from ~30 ns to ~80 ns (see e.g. [27,29] and [4] for a review). As the half time of this additional component is expected to lie in between that of the two main phases ascribed to PhQ reoxidation (25 ns and 250 ns respectively), imposing two lifetimes instead of the actual three results in a distribution of the additional component's DAS between the other two phases. Accordingly, both the 25-ns and 250-ns DAS of the PsaA–M688H/L mutants show a trough around 435 nm and, less distinctly, an additional peak around 350 nm (Fig. 2). Although the half time of the $P^+_{700}A^-_0$ charge recombination in the PsaA–M688H/L mutants cannot be determined accurately owing to the overlap with other components, the similar amplitudes of the two DAS at 440 nm would be indicative of a slightly longer half time than the ~30 ns reported for WT.

The increased probability of $P^+_{700}ec3^-_A$ decay via charge recombination could indicate a longer lifetime of $ec3^-_A$. This is consistent with the effect of this mutation as characterized by time-resolved EPR [18,25,30], ultra-fast spectroscopy [26,31] or absorption spectroscopy in the μs time domain [25]. These approaches led to the conclusion that the reoxidation of $ec3^-_A$ by PhQ_A is dramatically slowed down, if not blocked, in the PsaA–M688L/H mutants. In the analogous mutant in *Synechocystis* sp. PCC 6803, the EPR spectrum measured 150 ns after the flash displayed unusual features in the high-field region of the spectrum indicative of a long-lived $P^+_{700}A^-_0$ state [25]. Consistent with this, the yield of $^3P_{700}$ formation was significantly increased in this mutant [25]. We found that the ratio of the amplitude at 435 nm (where the contribution of PhQ^- is small) of the 6-μs DAS to that of the initial spectrum is ~75%. Thus, we estimate the fraction of centers that undergo $P^+_{700}A^-_0$ charge recombination to be ~25%, a figure that is smaller than that found with the analogous *Synechocystis* mutant [25]. This charge recombination process accounts, at least partly, for the apparently increased amplitude of the ~25-ns component in the PsaA–Met688 mutants. Indeed, by short circuiting ET down the A-branch, which bears the mutation, it *de facto* results in a higher *relative* reduction yield of PhQ_B and thus in a larger relative amplitude of the components assigned to its reoxidation.

In contrast to the $ec3_A$ mutants, there was no evidence for charge recombination in the PsaB–M668H mutant, as the initial spectrum was similar to the WT one, suggesting a similar total PhQ reduction yield. This is somewhat unexpected, since time-resolved EPR [18,30] and ultra-fast spectroscopy [31] studies consistently pointed to a significantly decreased rate of ET from $ec3^-_B$ to PhQ_B in these mutants. However, this may be a specific feature of the *Chlamydomonas* mutants, since analogous cyanobacterial mutants were indistinguishable from the WT by both techniques [25,32]. The faster/slower amplitude ratio observed in the PsaB–M668H mutant is very similar to the one found in the PsaB–Y676F mutant [24], where substitution of PsaB–Tyr676 for Phe lead to the loss of a hydrogen bond to $ec3_B$. By analogy, we propose that the PsaB–M668H mutation renders ET down the mutated branch less favorable and, in a compensatory manner, results in an increased probability for ET down the A-branch. The absence of charge recombination in the PsaB–M668H mutant may indicate that the two branches possess functional differences, which is a topic for future research.

3.2. The PsaA–S692A and PsaA–G693W mutants show retarded PhQ^-_A reoxidation and reveal a new 180-ns phase

According to the PS I structure ([1] and see Fig. 1), the hydroxyl group of the PsaA–Ser692 residue accepts a H-bond from the PsaA–Trp697 indole, which is itself π–π stacked with PhQ_A. As previously shown in *Synechocystis* sp. PCC 6803 [12,13], altering this stacking results in a considerable slowing down of the 250-ns component, which may be due to an alteration of the interaction between the indole and PhQ_A rings. The PsaA–G693W mutation was an attempt to make the vicinity of the PhQ binding pockets in the A and B branches more symmetric, as the residue corresponding to PsaA–Gly693 is a Trp in the B branch. In fact, it was recently hypothesized that this asymmetry explains the difference in rates of reoxidation of

PhQ_A and PhQ_B [33]. The fact that the PsaA–G693W mutation slows rather than accelerates ET from PhQ_A to F_X seems to disprove this hypothesis, but it seems likely that the introduction of an indole group would cause structural perturbations in the vicinity of the PhQ_A site, and this may be the main cause of the observed effect.

We observed a marked retardation of the slow nanosecond component ascribed to PhQ_A^- reoxidation in both the PsaA–S692A and PsaA–G693W mutants, and, more importantly, an additional component with a time constant of about 180 ns. The present results with the PsaA–S692A mutant are in good agreement with those previously reported for the cyanobacterial PsaA–S692C mutant [13], although the additional component was not reported there, presumably because the consequences of the mutation were analyzed at only two discrete wavelengths. The fortuitous and fortunate finding that two phases develop in well-separated time domains in the mutant was best established at 445 nm, where these two phases are associated with absorption changes of opposite sign (Fig. 3B) and where there is minimal contribution from the 25-ns and 6-μs components. This finding was strengthened by the similar trend observed in another mutant of the PhQ_A binding pocket, directly targeting the PsaA–W697 residue (PsaA–W697A, see Fig. 4). Taken together, these results suggest that the 180-ns component is not mutation-specific, but rather that it reflects a normally occurring process. Temporal overlap with the 250-ns component would obscure it in WT, allowing the mutations that slow $PhQ_A \rightarrow F_X$ ET to reveal it. The nature of the process represented by this new component will be discussed below.

3.3. Assignment of the 180-ns phase to ET from F_X to $F_{A/B}$

The DAS of the 180-ns phase shares no common features with the absorption changes associated with PhQ^- oxidation by the iron–sulfur clusters (see [34]). The shape of the bleaching in the 430–440 nm region might be taken as an indication that this component reflects the reduction of P_{700}^+ in a small fraction of PS I reaction centers. Based on its half time, this process is too fast to be assigned to P_{700}^+ reduction by an external electron donor and would thus reflect charge recombination between P_{700}^+ and either A_0^- or A_1^-. The former case is unlikely since the decay of the $P_{700}^+A_0^-$ radical pair is known to be significantly faster than ~180 ns (see discussion above). Under conditions where the F_X and $F_{A/B}$ clusters are reduced, a half time of 250 ns has been reported for the $P_{700}^+A_1^-$ charge recombination [35]. Yet, the negative feature in the 440–460 nm region makes the assignment of the ~180-ns component to charge recombination between P_{700}^+ or A_1^- unlikely since the spectroscopic signature of such charge recombination is expected to be a pronounced trough in the 430–440 nm region and a positive absorption in the 460 nm region [27,35], in contrast with our findings (Fig. 4). The broad trough in the 430-nm region and the small positive absorption increase in the near-UV part of the spectrum are instead reminiscent of the absorption changes associated with reoxidation of FeS clusters, as described originally by Hiyama and Ke [36]. Probably due to their very similar spectra, ET between FeS clusters has been difficult to observe directly by time-resolved absorption techniques. Even though the clusters are chemically identical, their environments are not, so absorption changes associated with ET between F_X^- and $F_{A/B}$ are not unlikely. Indeed, comparison of the absorption changes resulting from the formation of $P_{700}^+F_X^-$ and $P_{700}^+F_{A/B}^-$ revealed subtle differences. Lüneberg et al. found that the former are larger than the latter in the 340–400 nm region and smaller in the 450–480 nm region [37]. Based on the spectral features of the new component, we tentatively assign it to ET from F_X^- to $F_{A/B}$. We note that the resulting absorption changes may reflect this ET reaction either directly if the absorption changes associated with the redox changes of F_X and $F_{A/B}$ differ, or indirectly if this process induces electrochromic bandshift of the Chl or carotenoids nearby F_X.

Is the 180-ns time constant consistent with this assignment? To our knowledge, the present results would be the first direct measure of the ET rate between F_X^- and $F_{A/B}$. However, photovoltage measurements revealed a 220-ns phase with a relative amplitude that was too large (~30% of the overall electrogenicity) to be accounted for by ET between PhQ^- and F_X [38]. Removal of $F_{A/B}$ led to a ~60% reduction of the amplitude of this component with little change in rate. On this basis, Leibl and coworkers assigned this phase to ET between PhQ^- and $F_{A/B}$ and proposed that ET from PhQ^- to F_X was rate limiting. Similarly, Lüneberg et al. observed that depletion of the terminal $F_{A/B}$ clusters induced a slight decrease of the amplitude of the 250-ns component [37]. Here again, they proposed that ET from F_X^- to $F_{A/B}$ contributed to the overall absorption changes associated with this component and that it was faster than ET between PhQ^- and F_X. Recently, in model simulations based on electron transfer theory, the reoxidation of F_X^- was predicted to occur with an average lifetime of ~155 ns [6], in good agreement with the present value of 180 ns. It is of note that whereas the present proposal is made to account for the existence of an additional phase in the PsaA–S692A and PsaA–G693W mutants, these other approaches (photovoltage measurements, $F_{A/B}$ removal and theoretical calculations) dealt with WT PS I. This strongly suggests that ET between F_X^- and $F_{A/B}$ occurs in WT PS I with a time constant similar to the one found here (i.e. $\tau \approx 180$ ns) and that the mutation slowing down reoxidation of PhQ_A^- allowed observation of the inter-FeS ET by opening the time window during which it develops. As illustrated in Fig. 5, the fast nanosecond phase in WT would thus reflect the reoxidation of PhQ_B^- by F_X, while the slow nanosecond phase would encompass both ET from PhQ_A^- to F_X and ET from F_X^- to $F_{A/B}$. The mere fact that ET between the FeS clusters is observed *before* the reoxidation of PhQ_A^- (which is much slower in the PhQ_A pocket mutants) implies that an electron has reached F_X by another pathway (i.e. the B-branch), providing further independent support for the bidirectional model.

3.4. What could be the underlying explanation for the differences between the DAS of the faster and slower nanosecond components?

We now turn to the discussion of the DAS of the 25-ns and 250-ns components. These two phases are ascribed to the

reoxidation of PhQ_B^- and PhQ_A^-, respectively. In the absence of any charge recombination process short-circuiting PhQ reduction, the initial spectrum should be a linear combination of the ($P_{700}^+PhQ_A^-$–$P_{700}PhQ_A$) and ($P_{700}^+PhQ_B^-$–$P_{700}PhQ_B$) difference spectra, the contribution of these two spectra to the overall initial spectrum being weighted by the relative reduction yield of the two PhQs. If these spectra were very different, then mutations that change the relative weighting of the two spectra would result in an obvious shift in the shape of the initial spectrum closer to that of the dominant species. However, the initial spectra were similar in the WT and PsaB–M668H mutant, despite a significant change in the relative amplitude of the 25-ns and 250-ns components in the mutant with respect to WT (Fig. 2A). Similarly, the PsaA–Y696F and PsaB–Y676F mutations resulted in pronounced changes in the ratio between the fast and slow components, yet the initial spectra were similar [24]. This suggests that the (PhQ_A^-–PhQ_A) and (PhQ_B^-–PhQ_B) difference spectra are, within experimental accuracy, indistinguishable.

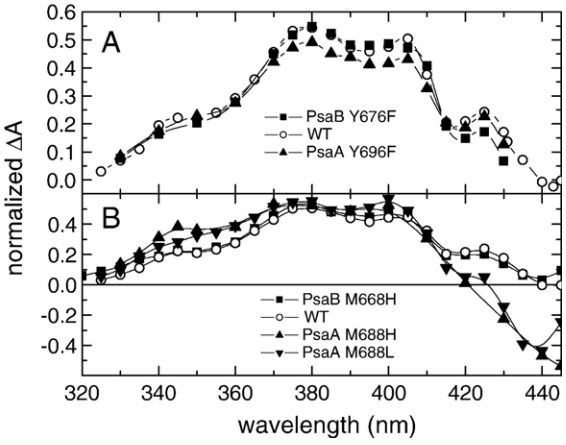

Fig. 6. Amplitudes (symbols) of total nanosecond absorption changes in *C. reinhardtii* cells in wild type samples (WT), and different ec3 mutants: PsaB–Y676F, PsaA–Y696F (Panel A) and PsaB–M668H, PsaA–M688H, PsaA–M688L (Panel B). Lines are just splines through the data points.

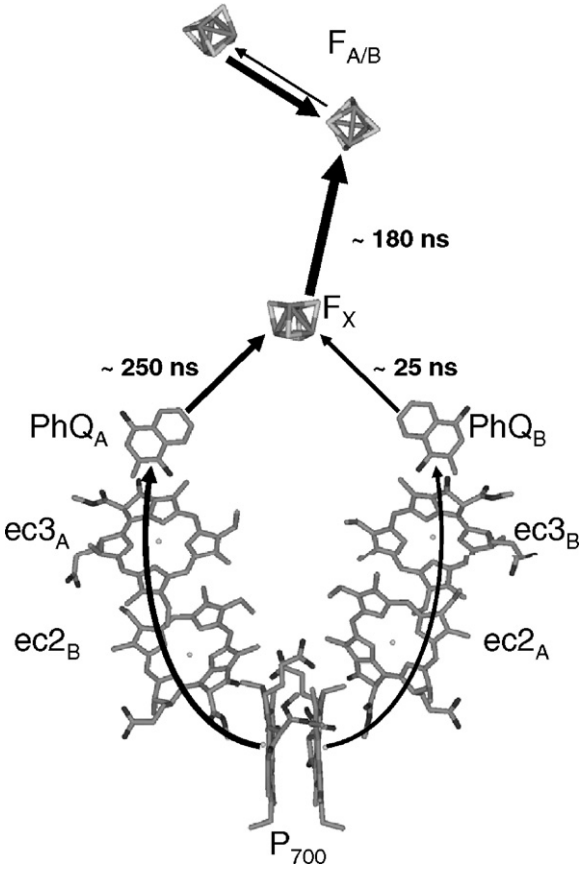

Fig. 5. A scheme depicting electron transfer in Photosystem I. Electron transfer may occur down both the A and B branch with different probabilities. Assuming that the absorption changes associated with the reoxidation of the two PhQs are similar at 380 nm (an assumption that is weakened by the finding of significantly different DAS for the fast and slow phases, see text for a discussion), these probabilities can be estimated from the relative amplitude of the 25-ns and 250-ns phases at 380 nm to be 0.6 for ET down the A-branch and 0.4 for ET down the B branch (as illustrated by the different thickness for the two arrows). As discussed in the text, ET between F_X^- and $F_{A/B}$ occurs with a time constant of ~180 ns. The indicated time constants correspond to apparent rather than intrinsic time constants of the individual steps, as equilibration between the various possible states is not taken into account here.

This problem can be approached from the other side by comparison of the spectra corresponding to the overall absorption changes taking place in the nanosecond time scales that is obtained by adding the DAS of the 25-ns and 250-ns components (Fig. 6). If our hypothesis concerning the 180-ns component holds true, then all of the changes occurring in this time scale encompass ET from both PhQs to F_X (25 ns, 250 ns) and from F_X to $F_{A/B}$ (180 ns). Again, if the (PhQ^-–PhQ) difference spectra were dramatically different between the two sides, then mutations that changed the ratio of PhQ_A^-/PhQ_B^- would skew the shape of this spectrum. However, they are remarkably similar to WT in the PsaA–Y696F, PsaB–Y676F, and PsaB–M668H mutants. The differences seen in the PsaA–M688H/L mutants are, as discussed above, due to the addition of the back-reaction component. Thus, we can conclude that the (PhQ^-–PhQ) difference spectra should be very similar between PhQ_A and PhQ_B.

However, there are clearly differences between the DAS of the fast and slow nanosecond phases (see Fig. 2), the most striking being the absence of the 340-nm peak in the fast phase. Moreover, changes in the amplitude of the slow phase provoked by the ec3 mutations are much stronger at wavelengths >360 nm than <360 nm. If the oxidation spectra of the PhQs (the electron donor) are similar, the most straightforward explanation for the DAS dissimilarities is that the reduction spectra of the electron acceptors are different. That is, the 25-ns component would reflect $PhQ_B^-F_X \rightarrow PhQ_BF_X^-$ for electrons originating from the B-branch. However, the 250-ns component in WT would correspond to the combination of $PhQ_A^-F_{A/B} \rightarrow PhQ_AF_{A/B}^-$ (200–250 ns) for electrons originating from the A-branch plus $F_X^-F_{A/B} \rightarrow F_XF_{A/B}^-$ (180 ns) for electrons originating from the B-branch. In the mutants where ET from PhQ_A^- is retarded, the latter ET event is sufficiently resolved to allow it to be observed, but note that the slowed component (750–1000 ns in the two mutants studied here) will still represent $PhQ_A^-F_{A/B} \rightarrow PhQ_AF_{A/B}^-$, and should still be

distinct from the 25-ns component. The removal of a fraction of the $F_X^- F_{A/B} \rightarrow F_X F_{A/B}^-$ component (due to electrons from the B-branch) in such mutants would be accompanied by less contribution of this spectrum to the DAS of the slowed component. In fact, the 1.1-μs DAS in PsaA–S692A and the 1.5-μs DAS in PsaA–G693W both have less positive amplitude in the 330–350 nm region and have more positive (less negative) amplitude in the 440–460 nm region, compared to WT (compare Fig. 4 to Fig. 2D). Although qualitatively consistent with the present hypothesis that part of the differences between the DAS of the two components ascribed to PhQ_A and PhQ_B reflects different electron acceptors, the amplitude of the component ascribed to ET between F_X^- and $F_{A/B}$ is too small, in the 340 nm region, to fully account for the pronounced shoulder in this wavelength region that is specific to the 250-ns DAS in the WT. Thus the possibility remains that this feature is, at least partly, also related to the reoxidation of PhQ_A^- rather than to ET between F_X^- and $F_{A/B}$.

There are other differences between the two nanosecond DAS that are not accounted for by differences between F_X and $F_{A/B}$. The most striking are the two peaks at 380 nm and 400 nm specifically observed in the 250-ns component DAS. Recently, Bautista et al. [16] have shown that the carotenoids and Chls undergoing electrochromic band-shift during the fast and slow phases have distinct spectroscopic properties. Similarly, Dobek and Brettel [17] observed that in *Synechocystis* WT, in the 690 nm region, the DAS of the fast and slow phases differ strongly and suggested that chlorophyll band-shifts may give rise to these spectral differences. By analogy, contributions from chlorophyll bandshifts in the blue cannot be excluded and might help to explain the two peaks which were consistently found in the DAS of the slow phase in PS I from *Chlamydomonas*, *Synechocystis* or *Chlorella* [11].

Acknowledgements

This work was supported in part by grants from the U.K. Biotechnology and Biological Sciences Research Council (BBSRC) (CO0350, CO7809 and B18658), the Leverhulme Trust (F/07134/N) and the European Union TMR program (Contract No. FMRX-CT98-0214) to P.H., and by a U.S. Dept. of Energy grant (DE-FG02-00ER15097) to K.R. S.S. wishes to thank Mike Evans (UCL, London) for stimulating discussion. M.B. acknowledges CNRS for financial support and thanks Klaus Brettel for helpful discussions.

References

[1] P. Jordan, P. Fromme, H.T. Witt, O. Klukas, W. Saenger, N. Krauss, Three-dimensional structure of cyanobacterial photosystem I at 2.5 A resolution, Nature 411 (2001) 909–917.
[2] A. Ben-Shem, F. Frolow, N. Nelson, Crystal structure of plant photosystem I, Nature 426 (2003) 630–635.
[3] P. Fromme, P. Jordan, N. Krauss, Structure of photosystem I, Biochim. Biophys. Acta 1507 (2001) 5–31.
[4] K. Brettel, Electron transfer and arrangement of the redox cofactors in photosystem I, Biochim. Biophys. Acta 1318 (1997) 322–373.
[5] K. Brettel, W. Leibl, Electron transfer in photosystem I, Biochim. Biophys. Acta 1507 (2001) 100–114.
[6] S. Santabarbara, P. Heathcote, M.C. Evans, Modelling of the electron transfer reactions in Photosystem I by electron tunnelling theory: the phylloquinones bound to the PsaA and the PsaB reaction centre subunits of PS I are almost isoenergetic to the iron–sulfur cluster F(X), Biochim. Biophys. Acta 1708 (2005) 283–310.
[7] P. Setif, Ferredoxin and flavodoxin reduction by photosystem I, Biochim. Biophys. Acta 1507 (2001) 161–179.
[8] F. Rappaport, B.A. Diner, K. Redding. in: J. Golbeck (Ed.). Photosystem I: The light Driven Plastocyanin ferredoxin oxidoreductase, Kluwer Academic Publishers (in press).
[9] P. Sétif, K. Brettel, Forward electron transfer from phylloquinone A_1 to iron sulfur centers in spinach photosystem I, Biochemistry 32 (1993) 7846–7854.
[10] A. Van Der Est, A.I. Valieva, Y.E. Kandrashkin, G. Shen, D.A. Bryant, J.H. Golbeck, Removal of PsaF alters forward electron transfer in photosystem I: evidence for fast reoxidation of QK-A in subunit deletion mutants of Synechococcus sp, PCC 7002, Biochemistry 43 (2004) 1264–1275.
[11] P. Joliot, A. Joliot, In vivo analysis of the electron transfer within photosystem I: are the two phylloquinones involved? Biochemistry 38 (1999) 11130–11136.
[12] M. Guergova-Kuras, B. Boudreaux, A. Joliot, P. Joliot, K. Redding, Evidence for two active branches for electron transfer in photosystem I, Proc. Natl. Acad. Sci. 98 (2001) 4437–4442.
[13] W. Xu, P.R. Chitnis, A. Valieva, A. van der Est, K. Brettel, M. Guergova-Kuras, Y.N. Pushkar, S.G. Zech, D. Stehlik, G. Shen, B. Zybailov, J.H. Golbeck, Electron transfer in cyanobacterial photosystem I: II. Determination of forward electron transfer rates of site-directed mutants in a putative electron transfer pathway from A0 through A1 to FX, J. Biol. Chem. 278 (2003) 27876–27887.
[14] S. Purton, D.R. Stevens, I.P. Muhiuddin, M.C. Evans, S. Carter, S.E. Rigby, P. Heathcote, Site-directed mutagenesis of PsaA residue W693 affects phylloquinone binding and function in the photosystem I reaction center of *Chlamydomonas reinhardtii*, Biochemistry 40 (2001) 2167–2175.
[15] K. Brettel, in: G. Garab (Ed.), Photosynthesis: Mechanism and Effects, vol. I, Kluwer Academic Publishers, 1998, pp. 611–614.
[16] J.A. Bautista, F. Rappaport, M. Guergova-Kuras, R.O. Cohen, J.H. Golbeck, J.Y. Wang, D. Beal, B.A. Diner, Biochemical and biophysical characterization of photosystem I from phytoene desaturase and zeta-carotene desaturase deletion mutants of *Synechocystis* sp. PCC 6803: evidence for PsaA- and PsaB-side electron transport in cyanobacteria, J. Biol. Chem. 280 (2005) 20030–20041.
[17] K. Dobek, K. Brettel, Photosynthesis: fundamental aspects to global perspectives, in: A. van der Est, D. Bruce (Eds.), Allen Press, Montréal, 2004, pp. 40–42.
[18] W.V. Fairclough, A. Forsyth, M.C. Evans, S.E. Rigby, S. Purton, P. Heathcote, Bidirectional electron transfer in photosystem I: electron transfer on the PsaA side is not essential for phototrophic growth in Chlamydomonas, Biochim Biophys. Acta 1606 (2003) 43–55.
[19] E.H. Harris, The Chlamydomonas Source Book, Academic Press, San Diego, 1989, pp. 413–433.
[20] Y. Li, M.G. Lucas, T. Konovalova, B. Abbott, F. MacMillan, A. Petrenko, V. Sivakumar, R. Wang, G. Hastings, F. Gu, J. van Tol, L.C. Brunel, R. Timkovich, F. Rappaport, K. Redding, Mutation of the putative hydrogen-bond donor to P700 of photosystem I, Biochemistry 43 (2004) 12634–12647.
[21] D. Béal, F. Rappaport, P. Joliot, A new high-sensitivity 10-ns time-resolution spectrophotometric technique adapted to in vivo analysis of the photosynthetic apparatus, Rev. Sci. Instrum. 70 (1999) 202–207.
[22] S. Grzybek, F. Baymann, K.-H. Müller, W. Mantele, Fifth international conference on the spectroscopy of biological molecules, in: T. Theophanides, J. Anastassopoulou, N. Fotopoulos (Eds.), Kluwer Academic Publishers, Dordrecht, 1993, pp. 25–26.
[23] M. Byrdin, R. Cohen, W.V. Fairclough, F. Gu, J. Golbeck, P. Heathcote, K. Redding, F. Rappaport, in: A. van der Est, D. Bruce (Eds.), Photosynthesis: Fundamental Aspects to Global Perspectives, Allen Press, Montréal, 2004, pp. 36–38.
[24] Y. Li, A. van der Est, M.G. Lucas, V.M. Ramesh, F. Gu, A. Petrenko, S.

Lin, A.N. Webber, F. Rappaport, K. Redding, Directing electron transfer within Photosystem I by breaking H-bonds in the cofactor branches, Proc. Natl. Acad. Sci. U. S. A. 103 (2006) 2144–2149.
[25] R.O. Cohen, G. Shen, J.H. Golbeck, W. Xu, P.R. Chitnis, A.I. Valieva, A. van der Est, Y. Pushkar, D. Stehlik, Evidence for asymmetric electron transfer in cyanobacterial photosystem I: analysis of a methionine-to-leucine mutation of the ligand to the primary electron acceptor A0, Biochemistry 43 (2004) 4741–4754.
[26] N. Dashdorj, W. Xu, P. Martinsson, P.R. Chitnis, S. Savikhin, Electrochromic shift of chlorophyll absorption in photosystem I from *Synechocystis* sp. PCC 6803: a probe of optical and dielectric properties around the secondary electron acceptor, Biophys. J. 86 (2004) 3121–3130.
[27] P.V. Warren, J.H. Golbeck, J.T. Warden, Charge recombination between $P700^+$ and A_1^- occurs directly to the ground state of P700 in a photosystem I core devoid of FX, FB, and FA, Biochemistry 32 (1993) 849–857.
[28] K. Brettel, M.H. Vos, Spectroscopic resolution of the picosecond reduction kinetics of the secondary electron acceptor A1 in photosystem I, FEBS Lett. 447 (1999) 315–317.
[29] H. Bottin, P. Sétif, Inhibition of electron transfer from A_0 to A_1 in photosystem I after treatment in darkness at low redox potential, Biochim. Biophys. Acta 1057 (1991) 331–336.
[30] S. Santabarbara, I. Kuprov, W.V. Fairclough, S. Purton, P.J. Hore, P. Heathcote, M.C. Evans, Bidirectional electron transfer in photosystem I: determination of two distances between P700+ and A1− in spin-correlated radical pairs, Biochemistry 44 (2005) 2119–2128.
[31] V.M. Ramesh, K. Gibasiewicz, S. Lin, S.E. Bingham, A.N. Webber, Bidirectional electron transfer in photosystem I: accumulation of A0- in A-side or B-side mutants of the axial ligand to chlorophyll A0, Biochemistry 43 (2004) 1369–1375.
[32] N. Dashdorj, W. Xu, R.O. Cohen, J.H. Golbeck, S. Savikhin, Asymmetric electron transfer in cyanobacterial Photosystem I: charge separation and secondary electron transfer dynamics of mutations near the primary electron acceptor A0, Biophys. J. 88 (2005) 1238–1249.
[33] N. Ivashin, S. Larsson, Electron pathways in photosystem I reaction centers, Chem. Phys. Lett. 375 (2003) 383–387.
[34] J.C. Romijn, J. Amesz, Purification and photochemical properties of reaction centers of *Chromatium vinosum*. Evidence for the photoreduction of a naphthoquinone, Biochim. Biophys. Acta 461 (1977) 327–338.
[35] P. Sétif, K. Brettel, Photosystem I photochemistry under highly reducing conditions: study of the P_{700} triplet state formation from the secondary radical pair ($P700^+A_1^-$), Biochim. Biophys. Acta 1020 (1990) 232–238.
[36] T. Hiyama, B. Ke, A further study of P430: a possible primary electron acceptor of photosystem I, Arch. Biochem. Biophys. 147 (1971) 99–108.
[37] J. Lüneberg, P. Fromme, P. Jekow, E. Schlodder, Spectroscopic characterization of PS I core complexes from thermophilic *Synechococcus* sp. Identical reoxidation kinetics of A_1− before and after removal of the iron–sulfur-clusters F_A and F_B, FEBS Lett. 338 (1994) 197–202.
[38] W. Leibl, B. Toupance, J. Breton, Photoelectric characterization of forward electron transfer to iron–sulfur centers in photosystem I, Biochemistry 34 (1995) 10237–10244.